ELECTROMAGNETIC MODES OF A COAXIAL PLASMA WAVEGUIDE IN AN EXTERNAL MAGNETIC FIELD

I.V. Karas', I.A. Zagrebelny
National Science Center "Kharkov Institute of Physics and Technology", Kharkov, Ukraine
E-mail: ira@kipt.kharkov.ua

For carrying out of the further numerical comparisons with experimental researches on breakdown of a mixture of gases by microwave radiation with a stochastic jumping phase the theoretical researches of wave dispersive properties of the coaxial waveguide are carried out. Electromagnetic modes of a coaxial plasma waveguide in an external magnetic field are investigated. The existence of quasi-TEM modes in a finite-strength magnetic field is demonstrated. It is shown that, in the limits of infinitely strong and zero magnetic fields, this mode transforms into a true TEM mode.

PACS: 52.80.Pi, 52.65.-y, 52.65.Ff, 52.70. Ds, 52.70.Kz, 84.40Fe

INTRODUCTION

For carrying out of the further numerical comparisons with experimental researches on breakdown of a mixture of gases by microwave radiation with a stochastic jumping phase [1 - 3] the theoretical researches of wave dispersive properties of the coaxial plasma waveguide are carried out in detail.

1. ELECTROMAGNETIC MODES OF A COAXIAL PLASMA WAVEGUIDE IN AN EXTERNAL MAGNETIC FIELD

In the theoretical study examines the axisymmetric waves that extended in the coaxial waveguide, which is filled a plasma, along the waveguide axis is applied an external constant magnetic field. Given the dependence of the components of the electric and magnetic fields of the coordinates and time has the form $A(\vec{x},t) = A(r)\exp[i(k_3 z - \omega t)]$ from Maxwell's equations for the matter we get the following equation system (compare with works [3, 4]):

$$k_3 E_\varphi = -kH_r\,,\ \frac{1}{r}\frac{\partial}{\partial r}(rE_\varphi) = ikH_z\,,$$

$$\frac{1}{r}\frac{\partial}{\partial r}(rH_\varphi) = -ik\varepsilon_3 E_z\,,\ ik_3 E_r - ikH_\varphi = \frac{\partial E_z}{\partial r}\,,$$

$$ik\varepsilon_1 E_r - ik_3 H_\varphi = k\varepsilon_2 E_\varphi\,,$$

$$ik\varepsilon_1 E_\varphi + ik_3 H_r - k\varepsilon_2 E_r = \partial H_z/\partial r\,, \quad (1)$$

$$k = \frac{\omega}{c},\ \varepsilon_1 = 1 - \frac{\omega_{pe}^2}{\omega^2 - \omega_{He}^2}\,,$$

$$\varepsilon_2 = -\frac{\omega_{pe}^2\omega_{He}}{\omega(\omega^2 - \omega_{He}^2)}, \varepsilon_3 = 1 - \frac{\omega_{pe}^2}{\omega^2}\,, \quad (2)$$

where $\omega_{pe} = \left(4\pi e_\alpha^2 n_0 / m_\alpha\right)^{1/2}$ is the electron Langmuir frequency, $\omega_{He} = e_\alpha H_0/(m_\alpha c)$ is the electron Larmor frequency.

2. TEM-TYPE MODES OF A COAXIAL PLASMA WAVEGUIDE WITHOUT AN EXTERNAL MAGNETIC FIELD

First, consider the system of equations (1) in the absence of an external magnetic field, i.e. ω_{He}=0, and accordingly ε_1=ε_3, ε_2=*0*.

$$k_3 E_\varphi + kH_r = 0\,,$$

$$ik_3 E_r - ikH_\varphi = \partial E_z/\partial r\,,$$

$$ik\varepsilon_1 E_\varphi + ik_3 H_r = \partial H_z/\partial r\,,$$

$$ik\varepsilon_1 E_r - ik_3 H_\varphi = 0\,, \quad (3)$$

$$\frac{1}{r}\frac{\partial}{\partial r}(rE_\varphi) = ikH_z\,,\ \frac{1}{r}\frac{\partial}{\partial r}(rH_\varphi) = -ik\varepsilon_1 E_z\,.$$

In this case, the system is divided into two systems of equations unrelated to describe the E- and H-wave. In the wave of E-type nonzero components of the electromagnetic field E_z, E_r, H_φ and *H*-type wave have the nonzero components H_z, H_r, E_φ. In a separate class you need to make waves in the TEM are zero z-component of the electric and magnetic fields.

We first look at the structure of TEM wave for which, by definition, [5] E_z = 0 and H_z = 0. From the equations (3) it follows:

$$E_\varphi = C_1/r\,,\ H_\varphi = C_2/r\,. \quad (4)$$

For the existence of waves is necessary to satisfy the boundary conditions, which in the case of coaxial waveguide are of the form:

$$E_z(a) = E_z(b) = 0,\ \ E_\varphi(a) = E_\varphi(b) = 0. \quad (5)$$

This means that the components of the field E_φ and correspondly H_r=-k_3/k·E_φ in TEM wave since no cannot be a solution in the form of (2.4) satisfy the boundary conditions (5). The nonzero components, defined by the formulas:

$$H_\varphi = \frac{C_2}{r}\,,\ E_r = \frac{k_3}{k\varepsilon_1}\frac{C_2}{r}\,. \quad (6)$$

The frequency of the wave is TEM from the dispersion equation:

$$k^2\varepsilon_1 - k_3^{\,2} = 0\,, \quad (7)$$

when $\omega \le \omega_{pe}$ TEM waves are absent, and when $\omega \ge \omega_{pe}$ a dispersion law has the form:

$$\omega^2 = k_3^2 c^2 + \omega_{pe}^2\,. \quad (8)$$

The dispersion curves for different values ω_{pe} shown in Fig. 1. Curve 1 corresponds to the zero-density plasma for its ε_1 = ε_3 = 1. In fact, the only wave coaxial vacuum waveguide and the frequency $\omega = k_3 c$. Curve 2 corresponds to ω_{pe}=1·10^{9}rad/s; 3 – ω_{pe} = 2·10^{9}rad/s; 4 - ω_{pe}= 2.5·10^{9}rad/s, 5 – ω_{pe}= 5.6·10^{9}rad/s.

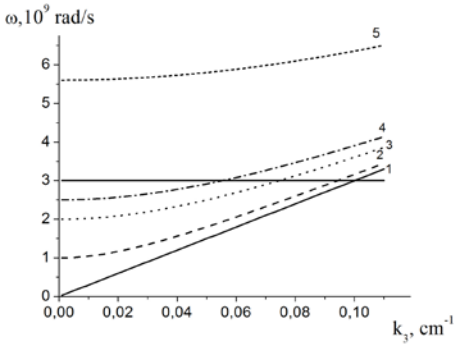

Fig. 1. The dispersion curves for different values of ω_{pe}

In experiments on the beam-plasma generator (BPG) signal is fed into the coaxial plasma waveguide with the main frequency $3\cdot10^9$ rad/s, which is marked by the horizontal line in Fig. 1. With increasing $k_3$thedispersion curves 2, 3, 4, and 5 converge closer to a curve 1, $\omega = k_3 c$.

Topography fields H_φ and E_r is shown in Fig. 2. In the middle are calculated for the case of the dispersion curve 3 in Fig. 1 ($\omega_{pe} = 2\cdot10^9$ rad/s) at the point $\omega = 3\cdot10^9$ rad/s. The curves are normalized to the value of the H_φ at $r = a = 0.6$ cm. It can be shown that the graphics fields H_φ and E_r in the vicinity of the intersection points corresponding-frequency signal with a straight $\omega = k_3 c$ will be very close.

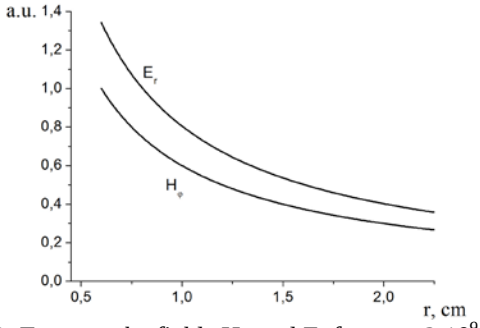

Fig. 2. Topography fields H_φ and E_r for $\omega_{pe}=2\cdot10^9$rad/s

From (6) and Fig. 2 shows that the field H_φ and E_r largest differ slightly for all radii and fall of hyperbole.

3. ELECTROMAGNETIC MODES OF A COAXIAL PLASMA WAVEGUIDE WITHOUT AN EXTERNAL MAGNETIC FIELD

Consider what else besides the TEM waves at the absence in waveguide of external-magnetic field. In this case the set equations (3) break up into two independent subsystems. The equation for the components of field H_r, E_φ,

$$H_z.\ \frac{\partial}{\partial r}\frac{1}{r}\frac{\partial}{\partial r}(rH_r) + (k^2\varepsilon_1 - k_3^2)H_r = 0,$$

$$\frac{\partial}{\partial r}\frac{1}{r}\frac{\partial}{\partial r}(rE_\varphi) + (k^2\varepsilon_1 - k_3^2)E_\varphi = 0. \quad (9)$$

Equations (9) in the case $k^2\varepsilon_1 - k_3^2 \neq 0$ are the equations for cylindrical (Bessel) functions of the first order Z_1 (λr). Their decision in the case of a two-connected domain (coaxial waveguide) is the combination of Bessel functions first and second kinds:

$$E_\varphi = C\left(J_1(\lambda r) + \overline{J_1(\lambda r)}\right) + B\left(N_1(\lambda r) + \overline{N_1(\lambda r)}\right), \quad (10)$$

where $\lambda = \sqrt{k^2\varepsilon_1 - k_3^2}$. Here C, B is arbitrary coefficients that are the boundary conditions. By the Bessel functions added someone complex-conjugate of the (horizontal bar over the function denotes complex conjugation) to condition real fields was performed for complex eigen values λ. Substitution E_φ, recorded thus in the boundary conditions (5) and taking into account that $\overline{J_1(\lambda r)} = J_1(\overline{\lambda} r)$ that allows us to obtain the dispersion-equation:

$$\begin{vmatrix} J_1(\lambda a) & N_1(\lambda a) \\ J_1(\lambda b) & N_1(\lambda b) \end{vmatrix} = 0. \quad (11)$$

Fig. 3 shows the solution of the dispersion equation for the following parameters of waveguide and plasma: a = 0.6 cm, b = 2.25 cm, $\omega_{pe}= 5.64\cdot10^9$ rad/s. The parameters taken for the real apparatus used in the experiment [2]. Type curves did not change with decreasing of plasma density and accordingly ω_{pe}, under big increasing of the plasma density the curves slightly lift up the ω.

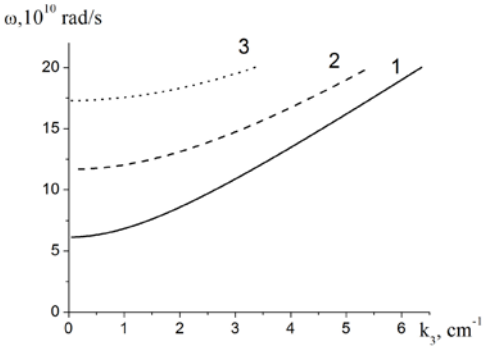

Fig. 3. The dispersion curves for the case $\omega_{pe} = 5.64\cdot10^9$ rad/s. The parameters of the waveguide: a = 0.6 cm, b = 2.25 cm. The numbers 1, 2, 3 are marked different radial waves

For the given geometrical dimensions of the waveguide and the plasma density is not solution at frequencies below $6.034\cdot10^{10}$ rad/s. For comparison, Fig. 4 shows the curves for the same parameters of the plasma but in the case where the outer radius of the waveguide b = 38.5 cm. At this case the lower curve in Fig. 4 at $k_3 = 0.013$ cm^{-1} corresponds to the frequency of the signal received from the BPG equal to $\omega = 3\cdot10^9$ rad/s.

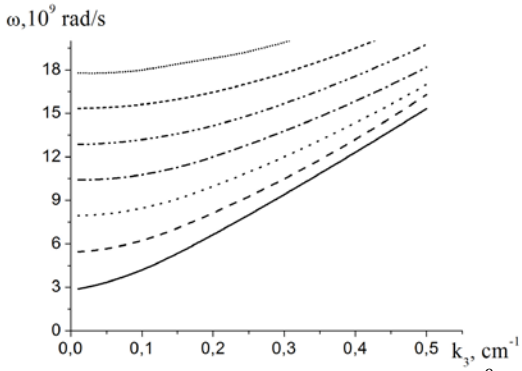

Fig. 4. Dispersion curves for the case $\omega_{pe}= 5.64\cdot10^9$ rad/s. Waveguide parameters: a= 0.6 cm, b = 38.5 cm

The following shows the radial distribution of components of the field for three dispersion curves shown in Fig. 5 at $\omega = 2\cdot10^{11}$ rad/s and respective k_3. We see that

for the first curve Fig. 5 the field distributions H_r, E_φ corresponds to one extreme point (maximum). For second curve is the two extreme points, for the third curve is three extreme points. The distribution of the field H_z for the first curve has no extreme points, for the second curve is one extreme point, for the third curve is the two extreme points.

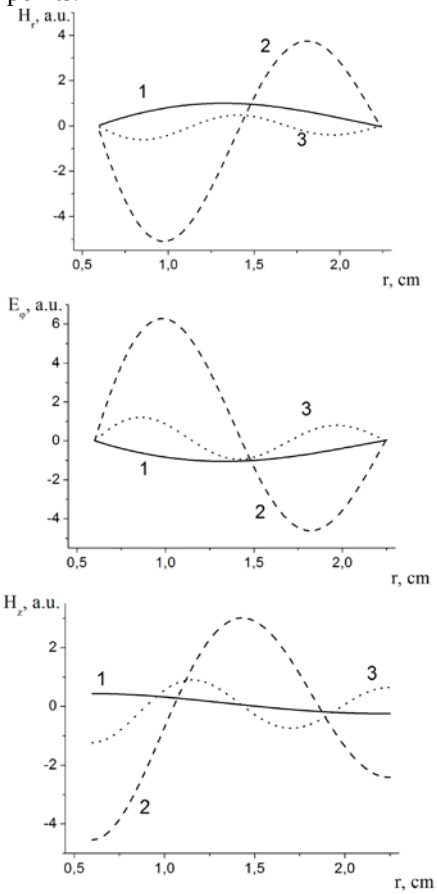

Fig. 5. Topography fields H_r, E_φ, H_z. The numbers 1, 2, 3 marked radial modes

The equations for components of E_r, H_φ, E_z fields.

$$\frac{\partial}{\partial r}\frac{1}{r}\frac{\partial}{\partial r}(rE_r)+(k^2\varepsilon_1-k_3^2)E_r=0,$$

$$\frac{\partial}{\partial r}\frac{1}{r}\frac{\partial}{\partial r}(rH_\varphi)+(k^2\varepsilon_1-k_3^2)H_\varphi=0. \quad (12)$$

Just as in the previous case, the solution of these equations is a combination of Bessel functions:

$$H_\varphi=C\left(J_1(\lambda r)+\overline{J_1(\lambda r)}\right)+B\left(N_1(\lambda r)+\overline{N_1(\lambda r)}\right). \quad (13)$$

Substituting into the equation of the system (3):

$$\frac{1}{r}\frac{\partial}{\partial r}(rH_\varphi)=-ik\varepsilon_1E_z.$$

Obtain an expression for E_z:

$$E_z=C\left(J_0(\lambda r)\right)+B\left(N_0(\lambda r)\right), \quad (14)$$

and after the satisfaction of the boundary conditions (5), we obtain the dispersion equation:

$$J_0(\lambda a)N_0(\lambda b)-J_0(\lambda b)N_0(\lambda a)=0. \quad (15)$$

The dispersion curves of the second triple of fields shown in Figs. 6, 7 shows the dispersion curves for the E-type wave (solid line) and H-type wave (dashed line). On Fig. 8 shows the radial distribution of the components of the field, three dispersion curves shown in Fig. 6 at $\omega = 2\cdot10^{11}$ rad/s and related k_3.

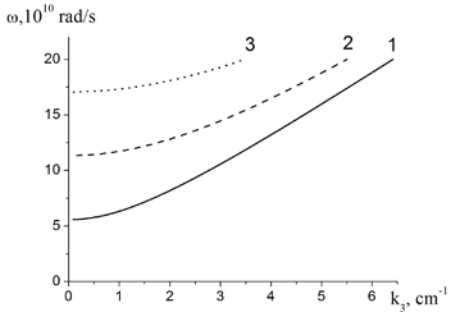

Fig. 6. The dispersion curves of the relation (15) for the case $\omega_{pe} = 5.64\cdot10^9$ rad/s. Parameters of waveguide are: a = 0.6 cm, b = 2.25 cm

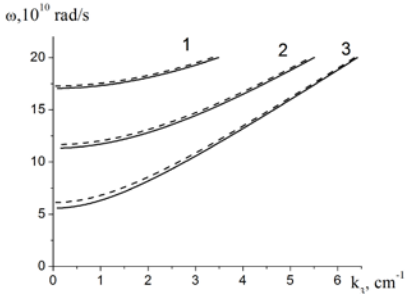

Fig. 7. Comparison of the dispersion curves for different triples fields. The dispersion relation (11) corresponds dashed line and the dispersion relation (15) corresponds solid line

We see that for the first curve of Fig. 6 the distribution of E_r, H_φ fields have not extreme points, for the second curve has one extreme point, for the third curve have the two extreme points. Allocation of E_z field for the first curve corresponds to one extremal point (maximum). The second curve have the two extreme points, the third curve have the three extreme points.

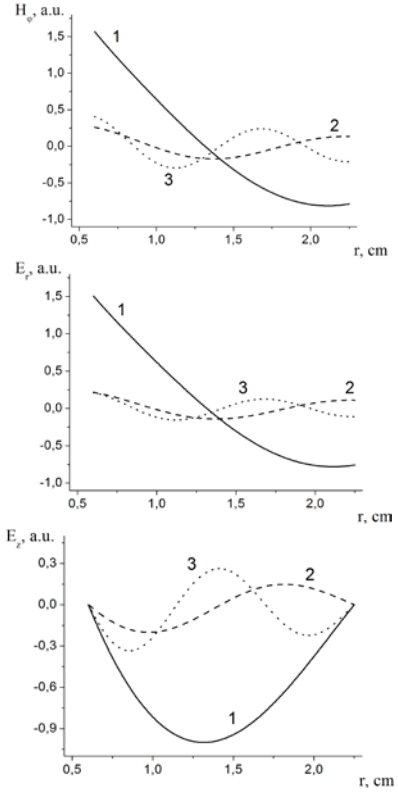

Fig. 8. Topography of E_r, H_φ, E_z fields. The numbers 1, 2, 3, marked radial modes corresponding dispersion curves in Fig. 6

4. ELECTROMAGNETIC MODES OF A COAXIAL PLASMA WAVEGUIDE IN AN EXTERNAL MAGNETIC FIELD

Let's go back to the original system of equations (1) and is considered to be at arbitrary values of the magnetic field and plasma density. In this case, the independent *E*-and *H*-type waves does not exist. Transforming the system of equations, we find the relationship between H_φ and E_φ, as well as between H_r and E_r:

$$\frac{\partial}{\partial r}\frac{1}{r}\frac{\partial}{\partial r}(rH_\varphi)+\frac{(k^2\varepsilon_1-k_3^2)\varepsilon_3}{\varepsilon_1}H_\varphi+kk_3\frac{\varepsilon_2\varepsilon_3}{\varepsilon_1}E_\varphi=0,$$

$$\frac{\partial}{\partial r}\frac{1}{r}\frac{\partial}{\partial r}(rE_\varphi)+(k^2\frac{\varepsilon_1^2+\varepsilon_2^2}{\varepsilon_1}-k_3^2)E_\varphi-kk_3\frac{\varepsilon_2}{\varepsilon_1}H_\varphi=0\,. \quad (16)$$

Set equations for H_r and E_r:

$$\frac{\partial}{\partial r}\frac{1}{r}\frac{\partial}{\partial r}(rH_r)+qH_r+sE_r=0\,, \quad (17)$$

$$\frac{\partial}{\partial r}\frac{1}{r}\frac{\partial}{\partial r}(rE_r)+pE_r+tH_r=0\,,$$

where $\tilde{\Delta}=\frac{\partial}{\partial r}\frac{1}{r}\frac{\partial}{\partial r}r$, $q=(k^2\varepsilon_1-k_3^2)$, $s=kk_3\varepsilon_2$,

$$p=[k^2(\frac{\varepsilon_2^2}{\varepsilon_1}+\varepsilon_3)-k_3^2\frac{\varepsilon_3}{\varepsilon_1}],\ t=[\frac{k^3}{k_3}\varepsilon_2(1-\frac{\varepsilon_3}{\varepsilon_1})-kk_3\frac{\varepsilon_2}{\varepsilon_1}].$$

This system of equations (17) is equivalent to two fourth-order equations for H_r and E_r:

$$\tilde{\Delta}^2H_r+(p+q)\tilde{\Delta}H_r+(qp-st)H_r=0\,, \quad (18)$$

$$\tilde{\Delta}^2E_r+(p+q)\tilde{\Delta}E_r+(qp-st)E_r=0\,. \quad (19)$$

From these equations it is seen that the radial components of the electric and magnetic fields are described by the same equation. The solution of the equation for H_r and E_r is the first order Bessel function $Z_1(\lambda r)$. It should be noted that $\tilde{\Delta}$ is not radial component of the transverse Laplacian operator, and a solution of both equations (18) is the first order Bessel function $Z_1(\lambda r)$. Substituting Z_1 (λr) in equation (18) we obtain an expression for the determination of λ:

$$\lambda^4-(p+q)\lambda^2+(qp-st)=0\,, \quad (20)$$

from its we find the values of λ^2:

$$\lambda_{1,2}^2=\frac{q+p}{2}\pm\sqrt{\frac{(q-p)^2}{4}+st}\,. \quad (21)$$

As can be seen from (21) generally have 4-root of equation (20):

$$\lambda_1=\sqrt{\frac{q+p}{2}+\sqrt{\frac{(q-p)^2}{4}+st}}\,,$$

$$\lambda_2=\sqrt{\frac{q+p}{2}-\sqrt{\frac{(q-p)^2}{4}+st}}\,,$$

$$\lambda_3=-\lambda_1=-\sqrt{\frac{q+p}{2}+\sqrt{\frac{(q-p)^2}{4}+st}}\,,$$

$$\lambda_4=-\lambda_2=-\sqrt{\frac{q+p}{2}-\sqrt{\frac{(q-p)^2}{4}+st}}\,.$$

The properties of the Bessel functions $Z_1(-\lambda r)=-Z_1(\lambda r)$ it should be that of Bessel functions for λ_1 and λ_3, as well as for λ_2 and λ_4 are linearly dependent. Therefore, the solution of the first equation (18) will be expressed by λ_1 and λ_2. In addition, as H_r is a real value, it will be limited to a combination of:

$$H_r=C\left(Z_1(\lambda_1 r)+\overline{Z_1(\lambda_1 r)}\right)+B\left(Z_1(\lambda_2 r)+\overline{Z_1(\lambda_2 r)}\right)\,. \quad (22)$$

Here C and B are the arbitrary coefficients, which are determined from the boundary conditions. Substituting H_r in the form (22) with the expression (21) for λ_1 and λ_2 and take into account the properties of Bessel functions $\overline{Z_1(\lambda r)}=Z_1(\bar{\lambda} r)$ as well as rules for their differentiation $Z_0'(\lambda r)=-\lambda Z_1(\lambda r)$, and obtain expressions for $\tilde{\Delta}H_r$ и $\tilde{\Delta}^2H_r$:

$$\tilde{\Delta}H_r=-C\left(\lambda_1^2Z_1(\lambda_1 r)+\bar{\lambda}_1^2Z_1(\bar{\lambda}_1 r)\right)-B\left(\lambda_2^2Z_1(\lambda_2 r)+\bar{\lambda}_2^2Z_1(\bar{\lambda}_2 r)\right),$$

$$\tilde{\Delta}^2H_r=C\left(\lambda_1^4Z_1(\lambda_1 r)+\bar{\lambda}_1^4Z_1(\bar{\lambda}_1 r)\right)+B\left(\lambda_2^4Z_1(\lambda_2 r)+\bar{\lambda}_2^4Z_1(\bar{\lambda}_2 r)\right).$$

After the substitution of which in the first equation (18) we get:

$$\tilde{N}\lambda_1^4Z_1(\lambda_1 r)+B\lambda_2^4Z_1(\lambda_2 r)-\tilde{N}\left[\lambda_1^2+\lambda_2^2\right]\lambda_1^2Z_1(\lambda_1 r)-$$
$$-B\left[\lambda_1^2+\lambda_2^2\right]\lambda_2^2Z_1(\lambda_2 r)+\lambda_1^2\lambda_2^2\left(\tilde{N}Z_1(\lambda_1 r)+BZ_1(\lambda_2 r)\right)+$$
$$+\tilde{N}\bar{\lambda}_1^4Z_1(\bar{\lambda}_1 r)+B\bar{\lambda}_2^4Z_1(\bar{\lambda}_2 r)-\tilde{N}\left[\lambda_1^2+\lambda_2^2\right]\bar{\lambda}_1^2Z_1(\bar{\lambda}_1 r)-$$
$$-B\left[\lambda_1^2+\lambda_2^2\right]\bar{\lambda}_2^2Z_1(\bar{\lambda}_2 r)+\lambda_1^2\lambda_2^2\left(\tilde{N}Z_1(\bar{\lambda}_1 r)+BZ_1(\bar{\lambda}_2 r)\right)=0.$$

Obviously, the first part of the expression-containing sponding part with λ equal to zero and after bringing the similar items have:

$$\tilde{N}\lambda_1^4Z_1(\lambda_1 r)+B\lambda_2^4Z_1(\lambda_2 r)-\tilde{N}\left[\lambda_1^2+\lambda_2^2\right]\lambda_1^2Z_1(\lambda_1 r)-$$
$$-B\left[\lambda_1^2+\lambda_2^2\right]\lambda_2^2Z_1(\lambda_2 r)+\lambda_1^2\lambda_2^2\left(\tilde{N}Z_1(\lambda_1 r)+BZ_1(\lambda_2 r)\right)=0.$$

The second part of the expression that contains the complex conjugate $\bar{\lambda}$ the solvable only if factors both at constant *C* and at constant *B* intercept to zero, that is:

$$C\bar{\lambda}_1^4Z_1(\bar{\lambda}_1 r)-C\left[\lambda_1^2+\lambda_2^2\right]\bar{\lambda}_1^2Z_1(\bar{\lambda}_1 r)+\lambda_1^2\lambda_2^2CZ_1(\bar{\lambda}_1 r)=0\,,$$

$$B\bar{\lambda}_2^4Z_1(\bar{\lambda}_2 r)-B\left[\lambda_1^2+\lambda_2^2\right]\bar{\lambda}_2^2Z_1(\bar{\lambda}_2 r)+\lambda_1^2\lambda_2^2BZ_1(\bar{\lambda}_2 r)=0\,.$$

And these conditions lead us to the fact that the complex conjugate parts $\bar{\lambda}_1$ and $\bar{\lambda}_2$ must satisfy the equations:

$$\bar{\lambda}_1^4-\left[\lambda_1^2+\lambda_2^2\right]\bar{\lambda}_1^2+\lambda_1^2\lambda_2^2=0\,, \quad (23)$$

$$\bar{\lambda}_2^4-\left[\lambda_1^2+\lambda_2^2\right]\bar{\lambda}_2^2+\lambda_1^2\lambda_2^2=0\,.$$

Which, in turn, means that:

$$\bar{\lambda}_1^2=\lambda_1^2\cup\lambda_2^2\,, \quad (24)$$

$$\bar{\lambda}_2^2=\lambda_1^2\cup\lambda_2^2\,.$$

From this we can conclude that we are entitled to write the expression for the field in the form:

$$H_r=CZ_1(\lambda_1 r)+BZ_1(\lambda_2 r).$$

In our case, we will conduct a review of coaxial waveguide with the conductive walls, which means solution will be put through a Bessel function and Neumann function, i.e.:

$$H_r=C_1J_1(\lambda_1 r)+C_2J_1(\lambda_2 r)+B_1N_1(\lambda_1 r)+B_2N_1(\lambda_2 r)\,. \quad (25)$$

Expressing E_φ and E_z by H_r written as (25), we obtain:

$$E_\varphi = \frac{-k}{k_3}\sum_{s=1}^{2}\left(C_s J_1(\lambda_s r) + B_s N_1(\lambda_s r)\right),$$

$$E_z = \frac{-i}{k_3\varepsilon_3}\sum_s \Lambda_s\left(C_s J_0(\lambda_s r) + B_s N_0(\lambda_s r)\right),$$

where

$$\Lambda_{1,2} = \frac{t\lambda_{1,2}\varepsilon_1}{p-\lambda_{1,2}^2} + \lambda_{1,2}\frac{k}{k_3}\varepsilon_2 . \qquad (26)$$

Satisfying the boundary conditions (5), we obtain the dispersion equation:

$$\begin{vmatrix} \Lambda_1 J_0(\lambda_1 a) & \Lambda_2 J_0(\lambda_2 a) & \Lambda_1 N_0(\lambda_1 a) & \Lambda_2 N_0(\lambda_2 a) \\ \Lambda_1 J_0(\lambda_1 b) & \Lambda_2 J_0(\lambda_2 b) & \Lambda_1 N_0(\lambda_1 b) & \Lambda_2 N_0(\lambda_2 b) \\ J_1(\lambda_1 a) & J_1(\lambda_2 a) & N_1(\lambda_1 a) & N_1(\lambda_2 a) \\ J_1(\lambda_1 b) & J_1(\lambda_2 b) & N_1(\lambda_1 b) & N_1(\lambda_2 b) \end{vmatrix} = 0. \qquad (27)$$

Below are shown the solution of the dispersion equation for the characteristic frequency with parameters corresponding to the experimental conditions. It should be noted that in some region on the plane (ω, k_3) square Eigen values λ (expression (21)) becomes complex. The boundaries of this region are determined by the condition that $(q-p)^2 + 4st < 0$, after substitution of values *q*, *p*, *s*, *t*, is given by:

$$\omega^4\left(\omega_H^2 + 4k_3^2c^2\right) - \omega^2\cdot 2k_3^2c^2\left(\omega_H^2 + 2\omega_p^2\right) + \\ + \omega_H^2 k_3^4 c^4 < 0.$$

The solution of this inequality leads to a condition on

$$\omega: \omega_2 < \omega < \omega_1,$$

$$\omega_{1,2} = k_3 c\left[\frac{2\omega_p^2 + \omega_H^2 \pm 2\left(\omega_p^4 + \omega_H^2\omega_p^2 - \omega_p^2 k_3^2 c^2\right)^{1/2}}{\omega_H^2 + 4k_3^2c^2}\right]. \qquad (28)$$

In this area, the Eigen values λ are complex conjugate, i.e. $\overline{\lambda_1} = \lambda_2$. Fig. 9 shows the dependence of the frequency ω vs. the longitudinal wave number $k_z = k_3$ when the electron-cyclotron frequency ω_{He} = 1.4·10^{10}rad/s. In Figs. 9 and 10 a complex λ^2 is limited lobe.

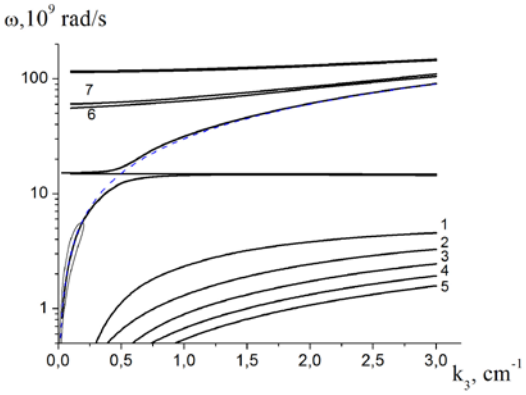

Fig. 9. The frequency ω of the longitudinal wave number k_3 in case ω_{pe} = 5.64·10^9 rad/s. The numbers represent the different branches of the plasma waves. For each of them a specific value λ: λ_1 = 1.86; λ_2 = 3.85; λ_3 = 5.7; λ_4 = 7.6; λ_5 = 9.5

The numbers (1) - (5) represent the different branches of high-frequency plasma waves. High-frequency plasma waves under given parameters of the waveguide and plasma are very close to the hybrid-frequency $\sqrt{\omega_{pe}^2 + \omega_{He}^2}$ and, for ease of analysis, are shown in a separate chart (Fig. 11). High-frequency and low-frequency TEM-type waves tend to ω = k_3c, which is highlighted in the chart the dashed blue line. Numerals (6) and (7) on the graph designated two first high-frequency electromagnetic waves. It can be seen that the branches of plasma waves with the increase in the value of k_3 is committed to ω_{pe} = 5.64·10^9 rad/s, but do not cross it. For ease of analysis Fig. 10 shows some dispersion curves, but on a linear scale, as opposed to Fig. 9, where the scale is logarithmic ω.

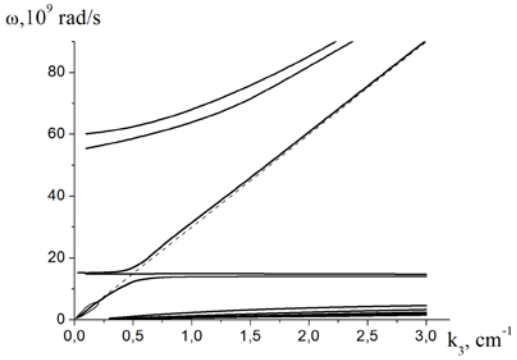

Fig. 10. The dependence of ω vs. k_3 at case ω_{pe} = 5.64·10^9 rad/s in the linear scale

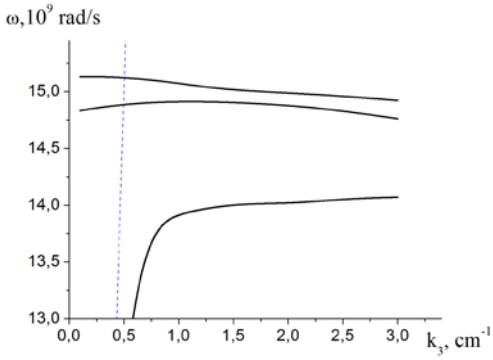

Fig. 11. The dependence ωvs. $k_3$for case ω_{pe} = 5.64·10^9 rad/s in the linear scale

Fig. 11 shows a part of Fig. 10 is an enlarged axially ω. It shows that near hybrid-frequency $\sqrt{\omega_{pe}^2 + \omega_{He}^2}$ are presented two branches of the high-frequency plasma waves. Here topography fields for this case. The expressions for the fields:

$$H_r = \sum_s (C_s J_1(\lambda_s r) + B_s N_1(\lambda_s r)),$$

$$E_\varphi = \frac{-k}{k_3}\sum_s (C_s J_1(\lambda_s r) + B_s N_1(\lambda_s r)),$$

$$E_z = \frac{-i}{k_3\varepsilon_3}\sum_s \Lambda_s (C_s J_0(\lambda_s r) + B_s N_0(\lambda_s r)),$$

$$E_r = \sum_s \frac{\lambda_s^2 - q}{s}\cdot (C_s J_1(\lambda_s r) + B_s N_1(\lambda_s r)),$$

$$H_\varphi = \sum_s \left[\frac{k\varepsilon_1}{k_3}\frac{\lambda_s^2 - q}{s} - \frac{k^2\varepsilon_2}{k_3^2}\right](C_s J_1(\lambda_s r) + B_s N_1(\lambda_s r)),$$

$$H_z = \sum_s \frac{-i\lambda_s}{k_3}(C_s J_0(\lambda_s r) + B_s N_0(\lambda_s r)),$$

$$E_z = \frac{-i}{k_3 \varepsilon_3} \sum_s \Lambda_s (C_s J_0(\lambda_s r) + B_s N_0(\lambda_s r)).$$

Fig. 12 shows the topography golf first radial threads plasma waves, (λ_1 = 1.86) and the waveguide parameters and plasma: a = 0.6 cm, b = 2.25 cm, $\omega_{pe} = 5.64 \cdot 10^9$ rad/s, $\omega_{He} = 1.4 \cdot 10^{10}$ rad/s. For convenience field analysis are normalized to the maximum value of H_r.

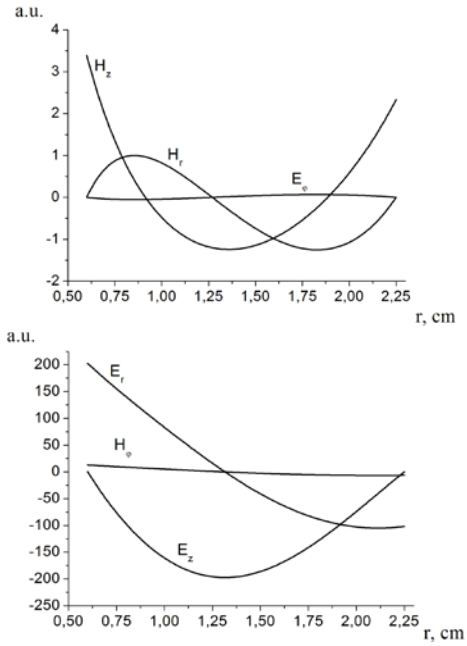

Fig. 12. Topography fields for the case λ_1= 1.86: curve 1 in Fig. 9 at $\omega = 4.6 \cdot 10^9$ rad/s, k_3 = 2.86. Parameters of the magnetic field and plasma density correspond $\omega_{pe} = 5.64 \cdot 10^9$ rad/s, $\omega_{He} = 1.4 \cdot 10^{10}$ rad/s

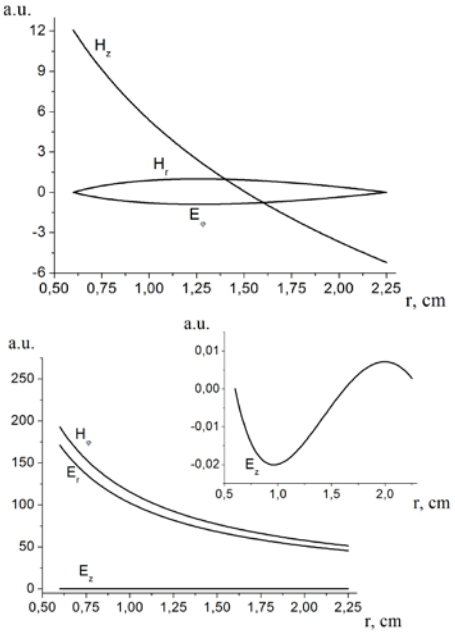

Fig. 13. Topography of low frequency fields for the caseterm TEM-wave at the point $\omega = 9 \cdot 10^9$ rad/s, $k_3 = 0.339$. The parameters of the magnetic field and plasma density correspond $\omega_{pe} = 5.64 \cdot 10^9$ rad/s, $\omega_{He} = 1.4 \cdot 10^{10}$ rad/s

This point corresponds to the phase velocity $\upsilon_{ph} = 2.65 \cdot 10^{10}$ cm / s, which is close to the light velocity c. As can be seen from figure 13 there are the dominant components of the field E_r, H_φ and H_z. The Umov-Poynting vector in the z direction for this wave is great because it is determined by $E_r \cdot H_\varphi$, $H_r \cdot E_\varphi$, the first of which is large.

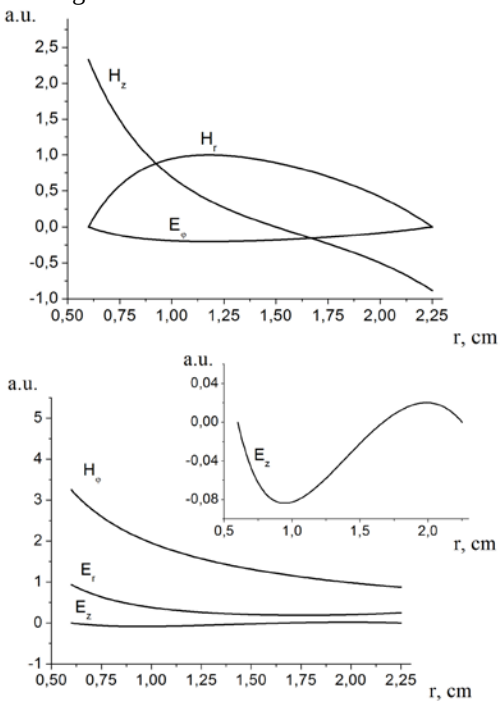

Fig. 14. Topography of low frequency fields for the case TEM-type wave at the point $\omega = 14 \cdot 10^9$ rad/s, $k_3 = 2.294$. The parameters of the magnetic field and plasma density correspond $\omega_{pe} = 5.64 \cdot 10^9$ rad/s, $\omega_{He} = 1.4 \cdot 10^{10}$ rad/s

This point corresponds to the phase velocity $\upsilon_{ph} = 6.1 \cdot 10^9$ cm / s, which is less than the light velocity c. As can be seen from Fig. 14 are dominant field component H_z, H_φ, H_r, E_r. The Umov-Poynting vector in the direction of z for this wave is not small, but significantly less than the point from Fig. 13.

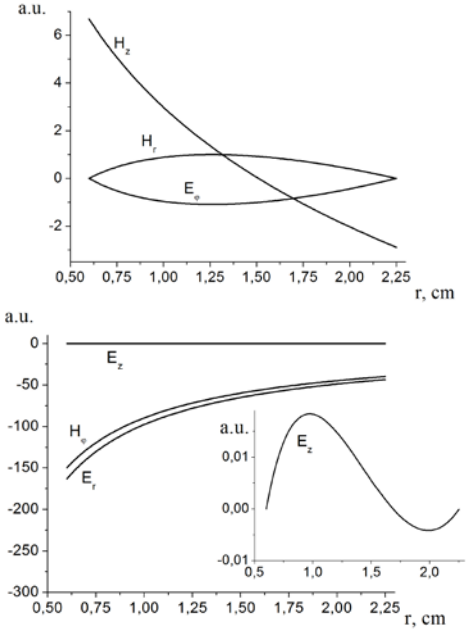

Fig. 15. Topography of fields for high-frequency TEM-type wave at the point $\omega = 2 \cdot 10^{10}$ rad/s, $k_3 = 0.613$. The parameters of the magnetic field and plasma density correspond $\omega_{pe} = 5.64 \cdot 10^9$ rad/s, $\omega_{He} = 1.4 \cdot 10^{10}$ rad/s

This point corresponds to the phase velocity $\upsilon_{ph}=3.26\cdot10^{10}$ cm/s, which is greater than the light velocity c. As can be seen from Fig. 15 are the dominant components of the field E_r, H_φ and H_z. The Umov-Poynting vector in the z direction for this wave is great because it is determined by $E_r \cdot H_\varphi$, $H_r \cdot E_\varphi$ the first of which is large.

CONCLUSIONS

For carrying out of the further numerical comparisons with experimental researches on breakdown of a mixture of gases by microwave radiation with a stochastic jumping phase the theoretical researches of wave dispersive properties of the created coaxial waveguide are carried out. Electromagnetic modes of a coaxial plasma waveguide in an external magnetic field are investigated. The existence of quasi TEM-type modes in a finite-strength magnetic field is demonstrated. It is shown that this mode transforms into the true TEM-mode under the limits of infinitely strong and zeros magnetic fields.

REFERENCES

1. V.I. Karas`, Ya.B. Fainberg, A.F. Alisov, A.M. Artamoshkin, R. Bingham, I.V. Gavrilenko, V.D. Levchenko, M. Lontano, V.I. Mirny, I.F. Potapenko and A.N. Starostin. Interaction of Microwave Radiation Undergoing Stochastic Phase Jumps with Plasmas or Gases // *Plasma Phys. Rep.* 2005, v. 31, № 5, p. 748-760.
2. V.I. Karas`, A.F. Alisov, A.M. Artamoshkin, S.A. Berdin, V.I. Golota, A.M. Yegorov, A.G. Zagorodny, I.A. Zagrebelny, V.I. Zasenko, I.V. Karas', I.F. Potapenko, and A.N. Starostin. Low Pressure Discharge Induced by Microwave Radiation with a Stochastically Jumping Phase // *Plasma Phys. Rep.* 2010, v. 36, № 8, p.736-749.
3. I.A. Zagrebelny, P.I. Markov, V.O. Podobinsky. About breakdown in a coaxial waveguide of atomic gas of low pressure by a microwave radiation with a stochastic jumping phase // *Problems of Atomic Sci. and Technol. Ser. "Plasma Electronics and New Acceleration Methods" (6).* 2008, v. 4(56), p. 195-198.
4. I.N. Kartashov, M.V. Kuzelev. Quasi-TEM Electromagnetic Modes of a Plasma Waveguide with a No simply Connected Cross Section in an External Magnetic Field // *Plasma Phys. Rep.* 2014, v. 40, № 12, p. 965-974.
5. L.D. Landau, E.M. Lifshits. *Electrodynamics of continuous media. Physical kinetics.* Moscow: "Nauka", 1982, 620 p.

Article received 20.05.2015

ВОЛНЫ В КОАКСИАЛЬНОМ ПЛАЗМЕННОМ ВОЛНОВОДЕ В МАГНИТНОМ ПОЛЕ

И.В. Карась, И.А. Загребельный

Для проведения дальнейших численных сравнений с экспериментальными исследованиями по пробою смеси газов с помощью микроволнового излучения со стохастическими скачками фазы проведены детальные теоретические исследования дисперсионных свойств плазменного коаксиального волновода. Исследованы электромагнитные волны, распространяющиеся в коаксиальном плазменном волноводе, помещенном во внешнее магнитное поле. Продемонстрировано наличие режимов квази ТЕМ-типа волн в магнитном поле конечной величины. Показано, что в пределах бесконечно сильного и нулевого магнитных полей существуют ТЕМ-типа волны.

ХВИЛІ В КОАКСІАЛЬНОМУ ПЛАЗМОВОМУ ХВИЛЕВОДІ В МАГНІТНОМУ ПОЛІ

І.В. Карась, І.А. Загребельний

Для проведення подальших кількісних порівнянь з експериментальними дослідженнями з пробою суміші газів за допомогою мікрохвильового випромінювання зі стохастичними стрибками фази проведені детальні теоретичні дослідження дисперсійних властивостей плазмового коаксіального хвилеводу. Досліджені електромагнітні хвилі, що поширюються в коаксіальному плазмовому хвилеводі, який вміщено в зовнішнє магнітне поле. Продемонстрована наявність режимів квазі ТЕМ-типу хвиль у магнітному полі скінченної величини. Показано, що в межах нескінченно сильного та нульового магнітних полів існують ТЕМ-типу хвилі.